Endocrinology, 2020, Vol. 161, No. 12, 1–16
doi:10.1210/endocr/bqaa201
Research Article

Research Article

GLP-1 Receptor Signaling Differentially Modifies the Outcomes of Sterile vs Viral Pulmonary Inflammation in Male Mice

Takehiro Sato,[1] Tatsunori Shimizu,[1] Hiroki Fujita,[1] Yumiko Imai,[2] Daniel J. Drucker,[3] Yutaka Seino,[4] and Yuichiro Yamada[1,4]

[1]Department of Endocrinology, Diabetes, and Geriatric Medicine, Akita University Graduate School of Medicine, Akita 010-8543, Japan; [2]Laboratory of Regulation for Intractable Infectious Diseases, Center for Vaccine and Adjuvant Research, National Institutes of Biomedical Innovation Health and Nutrition, Osaka 567-0085, Japan; [3]Department of Medicine, Lunenfeld-Tanenbaum Research Institute, Mt. Sinai Hospital, University of Toronto, Toronto M5G 1X5, Canada; and [4]Kansai Electric Power Medical Research Institute, Osaka 553-0003, Japan

ORCiD number: 0000-0003-1623-0815 (Y. Yamada).

Abbreviations: ATII, alveolar type II; cAMP, 3′,5′-cyclic AMP; GBP, guanylate-binding protein; GLP-1, glucagon-like peptide-1; GLP-1R, glucagon-like peptide-1 receptor; *Glp1r*$^{+/+}$, wild-type; *Glp1r*$^{-/-}$, GLP-1 receptor knockout; IL-6, interleukin-6; IRG, immunity-related guanosine triphosphatase; ISG, interferon-stimulated genes; KO, knockout; LPS, lipopolysaccharide; mRNA, messenger RNA; NF-κB, nuclear factor κB; NP, nuclear protein of influenza virus; qPCR, quantitative real-time polymerase chain reaction; T2D, type 2 diabetes; TNFα, tumor necrosis factor α.

Received: 14 September 2020; Editorial Decision: 23 October 2020; First Published Online: 30 October 2020; Corrected and Typeset: 20 November 2020.

Abstract

A number of disease states, including type 2 diabetes (T2D), are associated with an increased risk of pulmonary infection. Glucagon-like peptide-1 (GLP-1) receptor agonists are used to treat T2D and exert anti-inflammatory actions through a single, well-defined GLP-1 receptor (GLP-1R). Although highly expressed in the lung, little is known about the role of the GLP-1R in the context of pulmonary inflammation. Here we examined the consequences of gain or loss of GLP-1R activity in infectious and noninfectious lung inflammation. We studied wild-type mice treated with a GLP-1R agonist, and *Glp1r*$^{-/-}$ mice, in the setting of bleomycin-induced noninfectious lung injury and influenza virus infection. Loss of the GLP-1R attenuated the severity of bleomycin-induced lung injury, whereas activation of GLP-1R signaling increased pulmonary inflammation via the sympathetic nervous system. In contrast, GLP-1R agonism reduced the pathogen load in mice with experimental influenza virus infection in association with increased expression of intracellular interferon-inducible GTPases. Notably, the GLP-1 receptor agonist liraglutide improved the survival rate after influenza virus infection. Our results reveal context-dependent roles for the GLP-1 system in the response to lung injury. Notably, the therapeutic response of GLP-1R agonism in the setting of experimental influenza virus

ISSN Online 1945-7170

infection may have relevance for ongoing studies of GLP-1R agonism in people with T2D susceptible to viral lung injury.

Key Words: glucagon-like peptide-1 (GLP-1), lung inflammation, influenza

The lung is a complex organ, designed to facilitate gas and oxygen exchange, while preventing access of harmful noxious and infectious agents through a complex network of structural barriers and cellular defense systems (1, 2). Epithelial cells of the airway and alveoli and immune cells play central roles in lung barrier function. Epithelial cells act as a physical barrier while secreting mucus and antimicrobial peptides into the airway (3) as the first line of defense. Epithelial cells may also reduce infection by activating interferon-induced GTPases called guanylate-binding proteins (GBPs) (4) as the second line of defense, and secrete cytokines and chemokines to activate immune cell and to recognize and eliminate pathogens while reducing the extent of tissue damage as the third line of defense.

A distinct set of host responses are invoked by exposure of the lung to agents promoting chemical injury. When the lungs are exposed to toxic agents such as bleomycin, damaged pulmonary cells produce danger signals such as damage-associated molecular patterns (DAMPs), and immune cells are activated, contributing to repair of tissue damage, and lung remodeling (5). When infected with influenza virus, lung epithelial cells produce interferons and proinflammatory cytokines through the activation of pattern recognition receptors such as Toll-like receptor-3, Toll-like receptor-7, and retinoic acid-inducible gene-I (RIGI). Interferons in turn activate interferon-stimulated genes (ISGs), promoting cell host defenses that facilitate viral elimination through humoral and cellular immunity (6, 7).

A number of interacting systems contribute to control of immune activation within the lung, including the autonomic nervous system (8). The sympathetic nervous system may also contribute to organ homeostasis by modulating the immune system (9). Moreover the intestinal environment, exemplified by the gut microbiota and its metabolites, may also affect the susceptibility to lung inflammation through an emerging gut-lung axis (10, 11).

Gut hormones, exemplified by glucagon-like peptide-1 (GLP-1), are secreted from enteroendocrine L cells by nutrients, including short-chain fatty acids (12). Intriguingly, GLP-1 secretion is also controlled by microbial metabolites (13), and in turn, GLP-1 communicates locally with its receptor expressed on local intestinal intraepithelial lymphocytes (14, 15). GLP-1 attenuates experimental inflammation in preclinical studies and GLP-1 receptor (GLP-1R) agonists reduce systemic markers of inflammation in people with type 2 diabetes (T2D) (16). Notably, plasma levels of GLP-1 rise rapidly following the induction of experimental inflammation in humans (17), whereas GLP-1R-deficient mice exhibit enhanced sensitivity to chronic inflammation (18-20).

GLP-1Rs are expressed in the lung; however, the physiological importance of the pulmonary GLP-1R remains unclear (21-23). GLP-1 promotes secretion of pulmonary surfactant (24, 25), but whether these GLP-1 actions confer protection against inflammation-induced lung injury is not well established. A number of disease states are associated with increased risk of pulmonary infection, including T2D (26). The increased risk of influenza virus in people with T2D raises questions about whether different classes of glucose-lowering therapies might differentially attenuate inflammation-associated lung injury. Here we examined the importance of GLP-1 for the response to sterile bleomycin-induced lung injury and influenza virus infection in mice. Our findings support a role for activation of GLP-1R signaling in protection from influenza virus pulmonary injury. These actions are associated with activation of i) GBPs in lung epithelial cells and ii) danger signal-induced recruitment and activation of immune cells. Surprisingly, we see divergent effects of activating GLP-1R signaling in the 2 distinct lung injury models. Collectively, these results establish the GLP-1R as an additional component of an emerging gut-lung axis essential for control of a subset of biological responses to chemical- and pathogen-associated lung inflammation.

Materials and Methods

Animals

All animal care and experiments were approved by and conducted in accordance with protocols and guidelines of the Institutional Animal Care and Use Committee at the Akita University Graduate School of Medicine.

Wild-type (*Glp1r*$^{+/+}$) mice of C57BL/6 background were purchased from CLEA Japan, Inc, at age 6 to 7 weeks and maintained in a pathogen-free mouse facility until approximately age 9 to 10 weeks. GLP-1 receptor knockout (KO) (*Glp1r*$^{-/-}$) mice of C57BL/6 background were also maintained in a pathogen-free mouse facility. The generation of *Glp1r*$^{-/-}$ mice was described previously (27). No littermates were used in all experiments comparing wild-type and GLP-1R KO mice groups. All the mice used in the present study were male. Mice were anesthetized with an intraperitoneal injection of pentobarbital sodium (Sumitomo Dainippon Pharma, 50 mg/kg body weight), or a mixture of 3 anesthetics (medetomidine,

Nippon Zenyaku Kogyo, 0.6 mg/kg body weight; midazolam, Astellas, 4 mg/kg body weight; butorphanol, Meiji Seika Pharma, 5 mg/kg body weight) followed by subcutaneous administration of atipamezole (Nippon Zenyaku Kogyo, 0.6 mg/kg body weight), which is an α2 adrenergic receptor antagonist, as an anesthetic antagonist.

Bleomycin-induced lung injury model

At age approximately 9 to 10 weeks, mice were administered bleomycin hydrochloride (Nippon Kayaku, 2.5 mg/kg body weight) (28-30), in 50 μL of sterile phosphate-buffered saline by a single intratracheal injection after anesthesia. The GLP-1R agonists liraglutide (200 μg/kg body weight) were injected subcutaneously because previous in vivo experimentation has shown that 200 μg/kg body weight liraglutide causes an increase in tissue 3′,5′-cyclic AMP (cAMP) concentration (18). MR16-1, a neutralizing antibody against the murine interleukin-6 (IL-6) receptor, was kindly provided by Chugai Pharmaceutical (31). MR16-1 was administrated by a single intraperitoneal injection (2 mg/body weight) (32-34).

Influenza virus infection model

At the age of 9~10 weeks, mice were anesthetized and A/Puerto Rico/8/34 (H1N1; PR8) influenza virus (10 $TCID_{50}$/50 μL) was administered intratracheally to each mouse as described previously (35).

Histopathology of lung tissues

After thoracotomy, the lungs were perfused with phosphate-buffered saline and fixed with 4% paraformaldehyde. The lung samples were cut into 10-μm sections and stained with hematoxylin-eosin or Masson-Trichrome. In situ hybridization were performed using sense and antisense riboprobes directed against mouse *Glp1r* messenger RNA (mRNA) as described (18).

Collagen content of lung tissues

The frozen inferior lobe of the right lung was homogenized in 0.5 M acetic acid containing 1% pepsin (Sigma), and the lung collagen contents were measured using a Sircol collagen assay kit (Biocolor).

Isolation of CD45-positive and CD45-negative cells from murine lung

Briefly, 1 mL of dispase (BD Biosciences Discovery Labware) was instilled into the lungs via the trachea. The lungs were removed and incubated in a dispase-containing solution for 6 minutes at 37°C. The parenchymal tissue was carefully teased apart. The cells were passed through 40 μm of nylon cell strainers (BD Falcon) twice. After centrifuging cell suspension for 8 minutes at 130*g*, the cells were divided into CD45-positive and CD45-negative cells using CD45 microbeads (Miltenyi Biotec) (36) and an LS MACS separation column (Miltenyi Biotec).

Analysis of a lung epithelial cell line

The MLE12 mouse lung alveolar epithelial cell line (37) was obtained from ATCC and cultured with Dulbecco's modified Eagle's medium F12 (ATCC) supplemented with hydrocortisone (10 nM, Sigma), insulin (5 μg/mL, Sigma), transferrin (0.01 mg/mL, Sigma), β-estradiol (10 nM, Sigma), sodium selenite (30 nM, Sigma), HEPES (N-2-hydroxyethylpiperazine-N′-2-ethane sulfonic acid; 10 mM, Sigma), L-glutamine (2 mM, Gibco), fetal bovine serum (2%, HyClone Laboratories), and antibiotics (100 U/mL penicillin and 100 μg/mL streptomycin, Gibco) at 37°C in 5% CO_2. MLE12 cells were incubated with tumor necrosis factor α (TNFα; R&D, 100 ng/mL) and/or forskolin (Sigma, 10 μM) for 1 hour. H89 (Santa Cruz) was used at a concentration of 20 μM. 8-pCPT-2-O-Me-cAMP-AM (R&D) was used as an Epac activator at a concentration of 10 μM.

Quantitative real-time polymerase chain reaction

For quantitative real-time polymerase chain reaction (qPCR), total RNA was extracted from frozen middle lobes of the right lung using the RNeasy Mini kit (Qiagen). After reverse transcription was performed using the PrimeScript first-strand complementary DNA synthesis kit (Takara Bio), expression of each gene was assessed by qPCR using universal probe library assays (Roche Diagnostics) with predesigned probes and primers (Supplementary Table) (38). Ribosomal RNA (18S) expression was used for normalization.

Microarray analysis and pathway analysis

Lungs were excised from mice (age 9 weeks, n = 3 per group) 1 day after influenza virus infection and were used for microarray analysis. Briefly, total RNA was isolated using the RNeasy Mini kit, and microarray analysis was performed as described previously (39). A list of gene expression ratios and *P* values for the Welch *t* test derived from analysis of gene expression in the liraglutide-administered and nonadministered groups was imported into Ingenuity Pathways Analysis (Ingenuity). Data have been deposited

to the National Center for Biotechnology Information Gene Expression Omnibus (accession No.: GSE151886).

Statistical analysis

Paired and nonpaired *t* tests, one-way analysis of variance, and Mann-Whitney tests were performed with GraphPad prism 8, and log-rank tests were performed with SPBS, version 9.68.

Results

Bleomycin-induced lung injury is attenuated in *Glp1r*$^{-/-}$ mice

To investigate the role of endogenous GLP-1 signaling in the acute response to sterile lung inflammation, we administrated intratracheal bleomycin to GLP-1R-deficient (*Glp1r*$^{-/-}$) or wild-type (*Glp1r*$^{+/+}$) mice. The survival rates of *Glp1r*$^{-/-}$ and *Glp1r*$^{+/+}$ mice after bleomycin administration were similar as assessed at 2 weeks (Fig. 1A). Unexpectedly, *Glp1r*$^{-/-}$ mice exhibited less weight loss at 1 and 2 weeks after bleomycin instillation (Fig. 1B).

The pulmonary repair process after bleomycin administration is divided into acute inflammatory (days 0-3), proliferative (days 4-13), and remodeling phases (day 14). We evaluated the state of pulmonary inflammation during the acute inflammatory phase 2 days after bleomycin instillation. Interestingly, the relative induction of cytokine and chemokine mRNA transcripts was attenuated in bleomycin-treated *Glp1r*$^{-/-}$ vs *Glp1r*$^{+/+}$ mice (Fig. 1C). In the proliferative phase, the expansion of lung interstitium and associated infiltration of immune cells was also relatively reduced in *Glp1r*$^{-/-}$ compared to *Glp1r*$^{+/+}$ mice 1 week after bleomycin instillation (Fig. 1D). Moreover, mRNA transcripts encoding key molecular components of the proliferative pathway (40, 41) for epidermal growth factor receptor (*Egfr*) and transforming growth factor-β1 (*Tgfb1*) were expressed at lower levels in the lung of bleomycin-treated *Glp1r*$^{-/-}$ vs *Glp1r*$^{+/+}$ mice (Fig. 1E). We next evaluated the extent of lung fibrosis during the remodeling phase 2 weeks after bleomycin instillation. Histological findings showed that lung fibrosis in *Glp1r*$^{-/-}$ mice was comparatively modest (Fig. 1F), and collagen content in the lung was lower in *Glp1r*$^{-/-}$ vs *Glp1r*$^{+/+}$ mice (Fig. 1G). Moreover, levels of *Tgfb1* (42) mRNA transcripts were lower in lung RNA from *Glp1r*$^{-/-}$ vs *Glp1r*$^{+/+}$ mice (Fig. 1H). Collectively, these data reveal a reduced inflammatory and fibrotic response in the lungs of *Glp1r*$^{-/-}$ mice following bleomycin instillation.

Glucagon-like peptide-1 receptor agonists enhance bleomycin-induced lung inflammation

To assess the effects of activating the GLP-1 pathway on the development of acute lung inflammation, we administered liraglutide, a clinically approved GLP-1R agonist, to mice with bleomycin-induced lung injury. Unexpectedly, liraglutide produced a striking reduction in mouse survival after 2 weeks (Fig. 2A), associated with greater weight loss than observed in vehicle-treated mice (see Fig. 2A). Consistent with these findings, levels of mRNA transcripts for *Il6*, C-C motif chemokine 2 (*Ccl2*), interleukin-1β (*Il1b*), and C-X-C motif chemokine ligand 2 (*Cxcl2*), were increased in the lungs from the liraglutide-treated mice (Fig. 2B). Moreover, interstitial lung area was expanded in the liraglutide-treated mice after bleomycin administration (Fig. 2C).

Interestingly, the mortality of mice treated with liraglutide from 0 to 2 days was comparable with those of mice treated with liraglutide for 2 weeks after bleomycin administration (Fig. 2D).

Glucagon-like peptide-1 acts directly on alveolar type 2 epithelial cells to regulate cytokine expression

To identify the cellular targets of GLP-1 in the lung, we used in situ hybridization to localize GLP-1R mRNA within pulmonary cell types. *Glp1r* mRNA transcripts were detected in comparatively large-sized cells with a morphology consistent with alveolar type II (ATII) cells or alveolar macrophages (Fig. 3A). We isolated alveolar macrophages by bronchoalveolar lavage; however, *Glp1r* mRNA transcripts were not detected in RNA isolated from cellular components within bronchoalveolar lavage fluid (Fig. 3B). We then evaluated the expression levels of *Glp1r* mRNA in CD45-positive and CD45-negative cells. Through simultaneous examination of CD206 expression to identify macrophages, and surfactant protein C, a marker of ATII cells, we determined that *Glp1r* mRNA transcripts were localized to CD45-negative cells (Fig. 3C), suggesting that GLP-1Rs were expressed within ATII cells in the murine lung.

Although endogenous or pharmacological GLP-1R signaling modulated cytokine expression in the injured lung, the cells responsible for bleomycin and GLP-1R–dependent cytokine expression remained uncertain. We detected increased levels of *Il6* mRNA transcripts in RNA from CD45-negative cells isolated from *Glp1r*$^{+/+}$ but not from *Glp1r*$^{-/-}$ mouse lung 2 days after bleomycin instillation (Fig. 3D). Moreover, *Il6* mRNA levels were further upregulated by liraglutide treatment (see Fig. 3D). In contrast, *Il6* mRNA levels were at the lower limit of detection in CD45-positive cells and not different after bleomycin or liraglutide administration (see Fig. 3D). *Ccl2* mRNA levels were increased after bleomycin and further upregulated by liraglutide treatment both in CD45-negative and CD45-positive cells (see Fig. 3D). *Ccl2* mRNA levels were lower

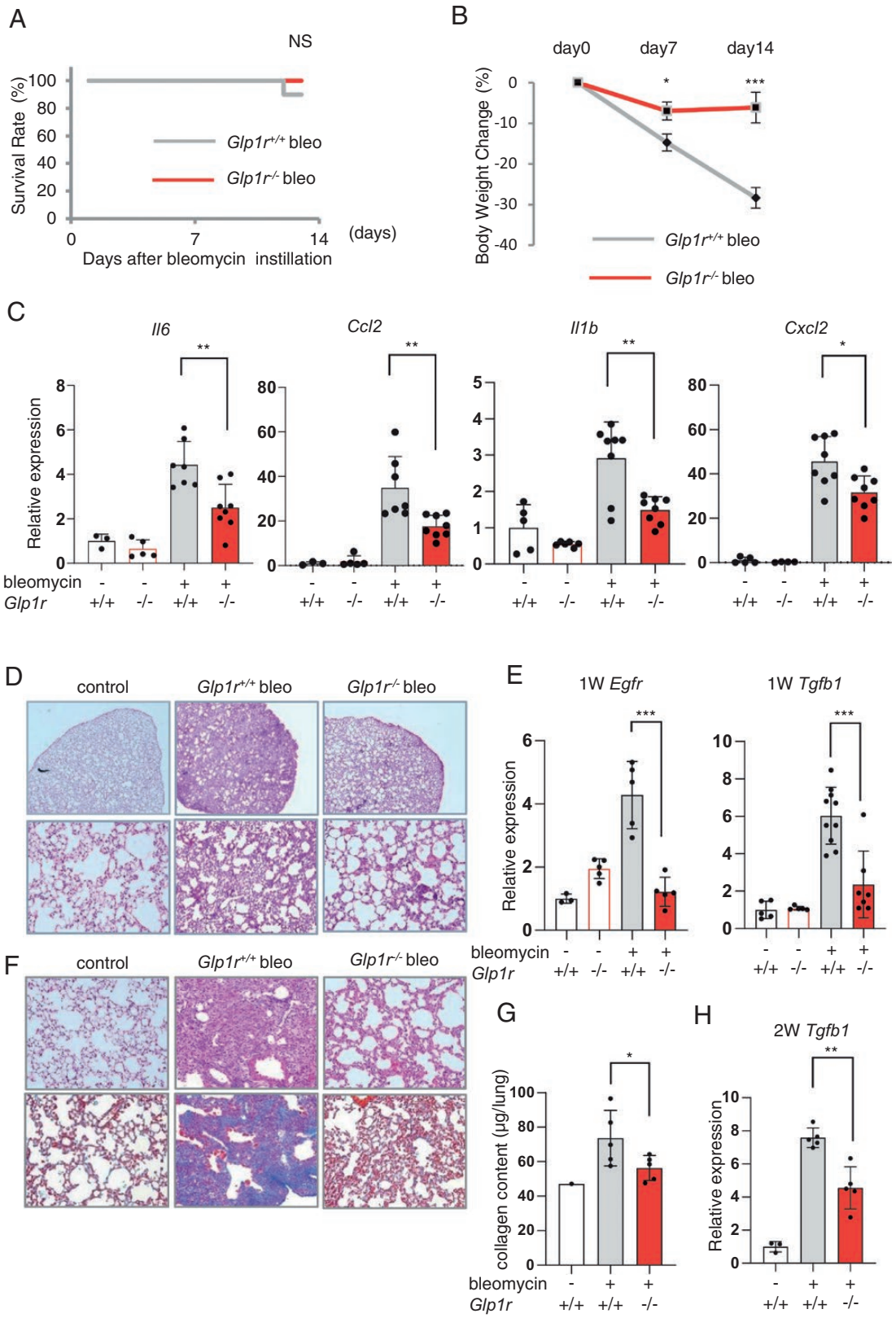

Figure 1. Bleomycin-induced lung injury in *Glp1r*$^{+/+}$and *Glp1r*$^{-/-}$ mice. A, Survival rates (each n = 10) and B, body weight changes (*Glp1r*$^{-/-}$: n = 11, *Glp1r*$^{+/+}$: n = 13) of *Glp1r*$^{-/-}$ mice and *Glp1r*$^{+/+}$ mice after intratracheal bleomycin instillation. C, Cytokines and chemokines gene expression in the lung 2 days after bleomycin instillation (n = 7~8), *Glp-1r*$^{-/-}$ without bleomycin (n = 4~5) or in the control lungs (n = 3). Control Ct values (interleukin-6 [IL-6], 35.8 ± 0.50; C-C motif chemokine 2 [CCL2], 38.6 ± 0.51; IL-1b, 31.4 ± 0.96; CXCL-2, 38.0 ± 0.98) D, Histological examination of hematoxylin-eosin staining 1 week after bleomycin. Upper panel: original magnification ×40, lower panel: original magnification ×200. E, *Egfr* (from left n = 3:5:5:5) and

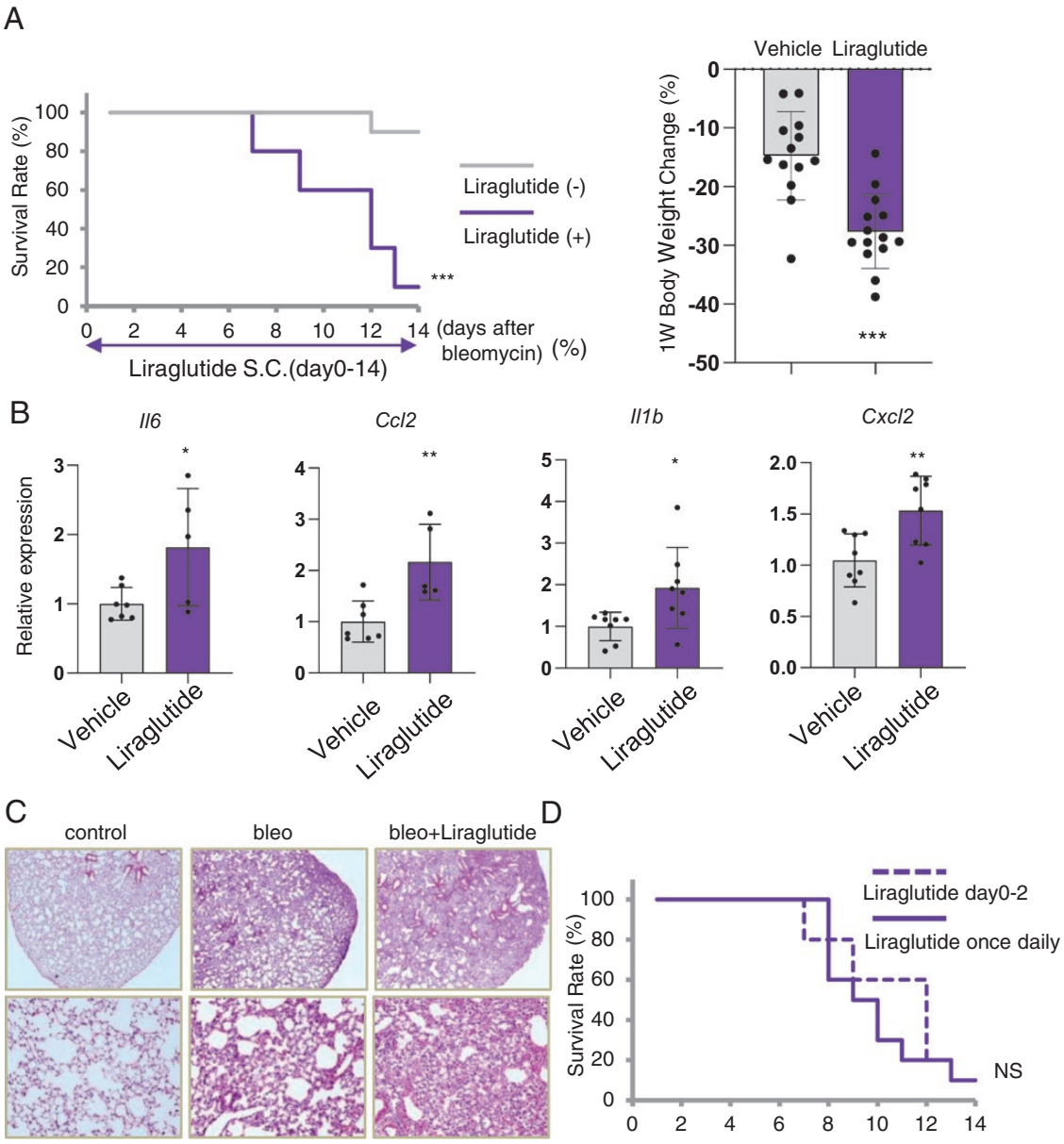

Figure 2. Bleomycin-induced lung injury is deteriorated by administration of a glucagon-like peptide 1 (GLP-1) receptor agonist. A, Survival rates (each n = 10) and body weight change (vehicle: n = 13, liraglutide: n = 14) of mice after intratracheal bleomycin instillation with or without liraglutide administration. B, Cytokine and chemokine gene expression in the lung 2 days after bleomycin instillation with or without liraglutide administration (vehicle: n = 7~8, liraglutide: n = 5~8). C, Histological examination of hematoxylin-eosin staining and 1 week after bleomycin instillation. Upper panel: original magnification ×40, lower panel: original magnification ×200. D, Survival rates of bleomycin-instilled mice medicated with liraglutide only days 0 to 2 after bleomycin or every day (each: n = 10). All values represent mean ± SEM **P* less than .05. ***P* less than .01. ****P* less than .001, not significant (NS) by A and D, log-rank test; or A and B, nonpaired *t* test.

in CD45-negative and CD45-positive cells from *Glp1r*$^{-/-}$ lung (see Fig. 3D).

Next, we examined regulation of cytokine expression using MLE12 cells, a murine ATII cell line (43). Because the nuclear factor (NF)-κB signaling pathway is activated in the bleomycin-induced lung injury model (42), we treated the MLE12 cells with TNFα, an activator of NF-κB. As GLP-1R signaling increases intracellular cAMP, but MLE12 cells do not express the GLP-1R, we treated the cells with forskolin, an adenylate cyclase activator.

Tgfb1 (from left n = 3:5:10:7) gene expression 1 week after bleomycin. F, Histological examination of hematoxylin eosin staining (upper panel) and Masson trichrome staining (lower panel) in the lung 2 weeks after bleomycin, original magnification ×200. G, Collagen content of the lung 2 weeks after bleomycin (from left n = 3:5:5). H, Transforming growth factor β1 (TGF-β1) gene expression 2 weeks after bleomycin (from left n = 3:5:5). All values represent mean ± SEM **P* less than .05. ***P* less than .01. ****P* less than .001 not significant (NS) by A, log-rank test; C, E, and H, one-way analysis of variance with multiple comparison test; or B and G, nonpaired *t* test.

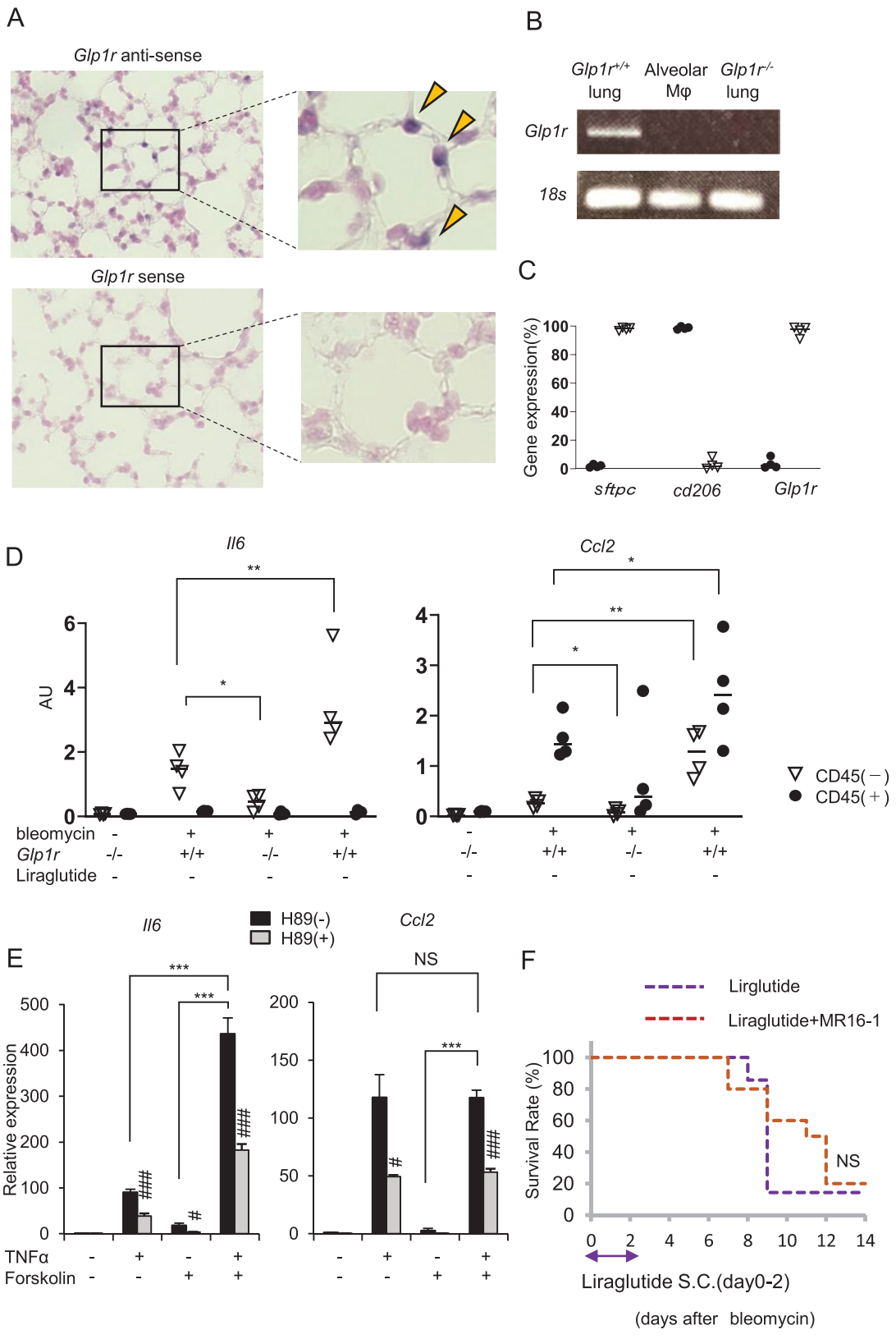

Figure 3. Glucagon-like peptide 1 (GLP-1) acts directly on type 2 alveolar epithelial cells to regulate cytokine expression. A, In situ hybridization analysis of murine lung using the antisense (upper) or sense (lower) probe for GLP-1 receptor messenger RNA (mRNA). B, Full-length *Glp1r* mRNA (upper) and partial 18S ribosomal RNA in the lung and alveolar macrophage. C, *Glp1r, Cd206*, and *Sftpc* mRNA transcripts in CD45-positive cells and CD45-negative cells from whole-lung cell suspension (each: n = 3). D, Gene expression of cytokine and chemokine in CD45-positive cells and CD45-negative cells from whole-lung cell suspension 2 days after bleomycin administration (each: n = 4). E, Gene expression of cytokine and chemokine

Levels of *Il6* and *Ccl2* mRNA transcripts were increased in response to TNFα, and the induction was partially attenuated by the protein kinase A inhibitor H89 (Fig. 3E). Moreover, the combination of TNFα and forskolin further increased the expression levels of *Il6* (but not *Ccl2*) to the extent of induction attenuated by H89 (see Fig. 3E). Interestingly, the combination of TNFα and forskolin also increased IL-6 promoter activity through H89-sensitive mechanisms (Supplemental Fig. 1A) (38) and double mutation of the NF-κB–responsive element (κB motif) and cAMP responsive element resulted in the complete loss of induction of IL-6 promoter activity by TNFα and forskolin (Supplemental Fig. 1B) (38). 8-pCPT-2-O-Me-cAMP-AM, a selective activator of the exchange protein directly activated by cAMP (Epac), did not increase IL-6 promoter activity (Supplemental Fig. 1A) (38).

Glucagon-like peptide-1 receptor agonism modulates lung inflammation via the sympathetic nervous system

Because liraglutide upregulated *Il6* expression in lungs after bleomycin administration, we assessed the importance of IL-6 in this model (44) using the anti–IL-6 receptor antibody MR16-1. No difference in survival was noted after bleomycin and liraglutide administration in the presence or absence of MR16-1 administration (Fig. 3F).

Next, we examined the potential role of the autonomic nervous system, known to convey GLP-1R–dependent signals (45-48), as an indirect mediator of GLP-1 action in the setting of bleomycin-induced lung injury (45-47) Using atipamezole, an α2 adrenergic receptor antagonist. Sympathetic blockade improved survival and attenuated body weight reduction in vehicle-treated mice administered bleomycin, and markedly reduced mortality and the extent of body weight reduction in liraglutide-treated mice with bleomycin lung injury (Fig. 4A and 4B). Furthermore, pulmonary levels of *Il6* and *Ccl2* mRNA transcripts were elevated following liraglutide administration but reduced in mice with concomitant sympathetic blockade (Fig. 4C). In contrast, levels of mRNA transcripts for *Il1b* and *Cxcl2* were not different across experimental groups (see Fig. 4C). The attenuation of lung congestion and inflammation after sympathetic blockade was also evident at the macroscopic and microscopic levels (Fig. 4D and 4E). These data indicate that the GLP-1R agonist liraglutide enhances bleomycin-induced lung inflammation through mechanisms requiring sympathetic nervous system activation.

Glucagon-like peptide-1 receptor agonist ameliorates influenza virus infection

To further probe the role of GLP-1R signaling in a different model of lung inflammation, we examined mice with experimental influenza virus infection. Remarkably, in contrast to findings in the sterile bleomycin injury model, liraglutide administration over 2 days improved the survival rate of influenza virus-infected mice (Fig. 5A). Levels of *Il6*, *Ccl2*, *Il1b*, and *Cxcl2* were higher in the lungs of mice with viral infection and reduced in liraglutide-treated mice (Fig. 5B). The levels of mRNA transcripts encoding the nuclear protein of influenza virus (NP), an indirect indicator of viral titer, were reduced in the lungs of liraglutide-treated mice (Fig. 5C). Interestingly, *Il6* and *Ccl2* mRNA levels were lower after influenza virus infection, whereas the ratios of *Il6/NP* and *Ccl2/NP* were increased by liraglutide, suggesting that liraglutide may also augment danger signal-induced recruitment and activation of immune cells after influenza virus infection (Fig. 5D).

We next examined the consequences of influenza virus infection in GLP-1R–deficient mice. In contrast to data obtained with pharmacological GLP-1R agonism, cytokine and *NP* expression, body weight, and survival were not different in $Glp1r^{-/-}$ vs $Glp1r^{+/+}$ mice with influenza virus infection (Supplemental Fig. 2) (38). Moreover, sympathetic blockade did not alter the effect of liraglutide on survival in mice with influenza infection (Supplemental Fig. 3) (38).

Glucagon-like peptide-1 receptor agonism increases the expression of interferon-inducible GTPases

To investigate how liraglutide promotes resistance against the inflammatory sequelae activated by the influenza virus, we examined gene expression in the lung after influenza virus infection using microarray analysis. In the pathway analysis, expression of genes contributing to interferon signaling were increased in the lung the first day after influenza virus infection (Supplemental Fig. 4A) (38). Therefore, we next analyzed the expression of a subset of ISGs (49) (Fig. 6A). We detected increased expression of several members of the interferon-inducible GTPases,

in the MLE12 1 hour after medication. Black bar: without H89, gray bar: with H89 (each n = 4). F, Survival rates of mice after intratracheal bleomycin instillation with liraglutide medicated with or without MR16-1 (without MR16-1, n = 7; with MR16-1,n = 10). All values represent mean ± SEM. **P* less than .05. ***P* less than .01. ****P* less than .001 Not significant (NS) by one-way analysis of variance (ANOVA) with D and E, multiple comparison test; or F, log-rank test. In Fig. 3E, # *P* less than .05, ###*P* less than .001 vs absence of H89 by one-way ANOVA with multiple comparison test.

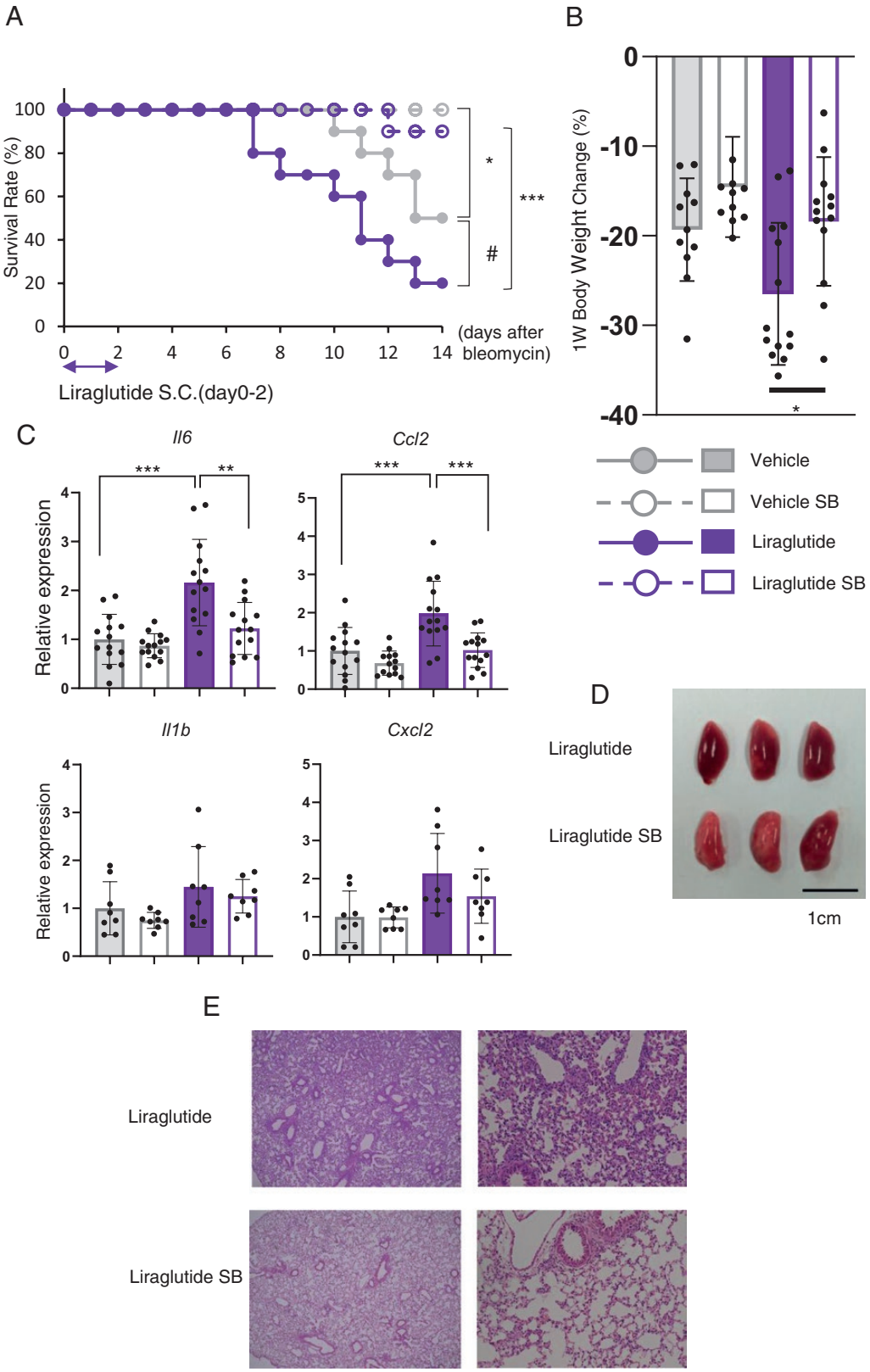

Figure 4. Glucagon-like peptide 1 receptor (GLP-1R) agonism enhances sterile lung inflammation via the sympathetic nervous system. A,The effect of chemical sympathetic nerve blockade on survival rates (each: n = 10) and B, body weight change (from left n = 11:11:14:13) of mice after intratracheal bleomycin instillation with or without liraglutide administration. C, Cytokines and chemokines gene expression (interleukin-6 [*Il6*], *CCl2,* n = 13~14 *Il1b, Cxcl2,* n = 8) in the lung 2 days after bleomycin instillation. D, Gross lung (upper lobe of lung) finding 1 week after bleomycin instillation. E, Histological examination of hematoxylin-eosin staining and 1 week after bleomycin instillation. Upper panel: non-SB group with liraglutide, lower panel: SB group with liraglutide. Left panel: original magnification ×40. Right panel: original magnification ×200. All values represent mean ± SEM. **P* less than .05, ***P* less than .01, ****P* less than .001 by A, log-rank test; or B and C, one-way analysis of variance with multiple comparison test.

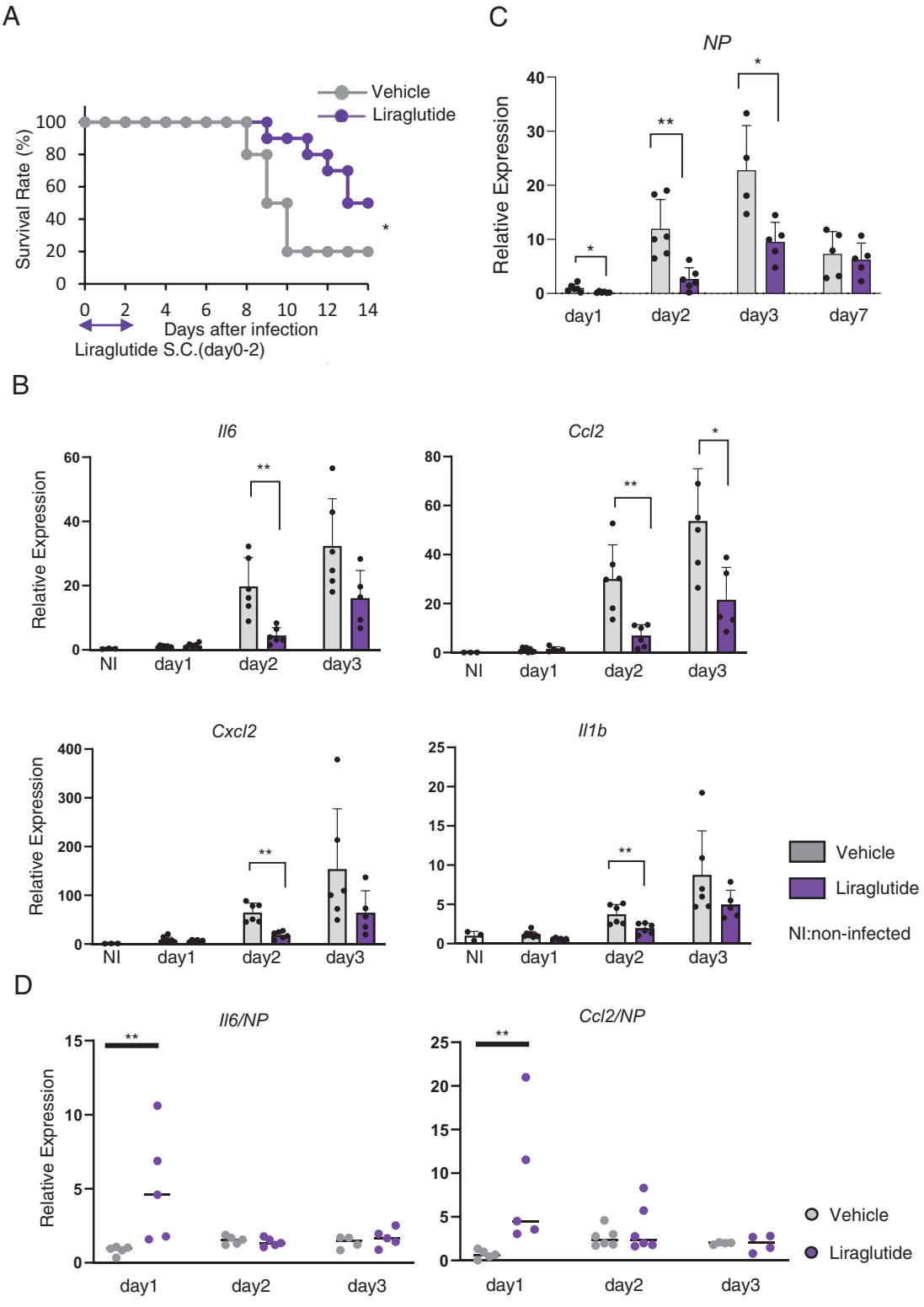

Figure 5. The glucagon-like peptide 1 receptor (GLP-1R) agonist liraglutide ameliorates influenza virus infection. A, Survival rates of mice after influenza virus infection with or without liraglutide administration (each n = 10). B, Cytokine and chemokine gene expression in the lung after influenza virus infection (from left interleukin-6 [*Il6*]: n = 3:8:6:6:6:6:5, *Ccl2*: n = 3:8:5:6:6:6:5, *Cxcl2*:n = 3:8:6:6:6:6:5, *Il1b*:n = 3:8:6:6:6:6:5). C, *NP* messenger RNA transcripts in the lung after influenza virus infection (from left n = 6:6:6:6:4:5:6:6). D, *Il6/NP* (from right n = 5:5:5:5:4:5) and *Ccl2*/*NP* (from left n = 5:5:6:6:4:4) ratios in the lung after influenza virus infection. B and C, Values represent mean ± SEM. D, Value represents median. **P* less than .05. ***P* less than .01 by A, log-rank test; B and C, one-way analysis of variance with multiple comparison test; or D, Mann-Whitney test.

GBPs, in lung tissue from liraglutide-treated mice with experimental influenza virus infection. These findings prompted us to examine expression levels of other GBPs (7). Levels of mRNA transcripts for several members of the immunity-related guanosine triphosphatase (IRG) family, GBP family, and very large interferon-inducible GTPase family were selectively increased in liraglutide-treated mice (Fig. 6B). Interferon-γ–induced GTPase (*Igtp*) and T-cell specific GTPase 2 (*Tgtp2*), members of the IRG family not included in the analysis shown in Fig. 6A, were increased by influenza virus infection and further induced by liraglutide treatment (Fig. 6C). In contrast, levels of myxovirus resistance 1 (*Mx1*), a gene encoding a component of the antiviral response, were lower with liraglutide administration (Supplemental Fig. 5A) (38) and were correlated with influenza virus load as approximated by NP expression (Supplemental Fig. 5B) (38). Nevertheless, the *Mx1*/*NP* ratio was increased in liraglutide-treated mice (Supplemental Fig. 5C) (38). Although there was no difference in the expression of most interferon genes with liraglutide treatment (Fig. 6D, Supplemental Fig. 4B) (38), *Ifna1* levels were higher and interferon regulatory factor 1 (*Irf1*) and interferon regulatory factor 9 (*Irf9*), which are transcription factors involved in stimulating ISG gene expression interferon independently, were increased after liraglutide administration (Fig. 6D and 6E). These data suggest that enhanced expression of the GBPs by liraglutide may contribute to augmenting a subset of the interferon response enabling increased resistance to influenza virus infection.

Discussion

The secretion of GLP-1, a hormone secreted from the intestinal tract, is known to be induced by inflammatory stimuli, including microbial metabolites, and lipopolysaccharide (LPS) (50, 51). Indeed, levels of GLP-1 rise rapidly in humans after LPS administration (17), and higher levels of circulating GLP-1 correlate with adverse outcomes in hospitalized patients with critical illness, notably individuals with sepsis admitted to the intensive care unit (52). These findings are consistent with the notion that the L cell is a pathogen sensor, and activates GLP-1 secretion in response to inflammation.

Here we analyzed the importance of endogenous and pharmacological GLP-1 action in 2 distinct mouse models of lung inflammation: (1) chemical toxicity induced by bleomycin, an agent known to produce oxidative damage in the human lung, and (2) influenza virus infection. We found that disruption of endogenous GLP-1R signaling improved outcomes in mice with bleomycin-induced lung injury, but is not important for the response to influenza virus infection. In contrast, pharmacological activation of GLP-1R signaling with liraglutide exacerbated outcomes in the bleomycin model, yet reduced mortality in mice with influenza virus infection. These divergent findings highlight the importance of studying substantially different models of lung injury for gaining insights into the intersection of GLP-1R signaling and tissue inflammation. Our findings suggest that GLP-1R signaling protects the lung from influenza infection via 2 lines of defense, activation of GBPs in lung epithelial cells and danger signal–induced recruitment and activation of immune cells (Fig. 7).

These observations raise multiple hypotheses for mechanisms linking GLP-1R signaling to the extent of pulmonary inflammation. GLP-1 may act directly on local GLP-1R–positive cells to enhance cytokine and chemokine production. Indeed, liraglutide increased *Il6* gene expression in CD45-negative cells after bleomycin-induced lung injury, which included ATII cells. Moreover, canonical GLP-1 signaling activates G_s–coupled pathways, notable in the context of our findings in that forskolin-activated cAMP signaling promoted *Il6* expression alone and in combination with TNFα. These results are consistent with the possibility that GLP-1 acts directly on alveolar epithelial cells in vivo, as postulated in the context of LPS-induced lung injury (53). Mechanistically, although IL-6 expression was induced by liraglutide administration, IL-6 receptor blockade had no effect on the mortality rate in liraglutide-treated mice with bleomycin-induced lung injury. Although GLP-1–induced IL-6 elevation may contribute to the inflammatory process in some settings, our data suggest that IL-6–independent mechanisms likely mediate bleomycin-induced mortality.

Alternatively, liraglutide may act indirectly to modify bleomycin-induced lung injury through the autonomic nervous system. Various studies have revealed that the autonomic nervous system plays an important role in the regulation of inflammation and GLP-1 modulates the activity of the autonomic nervous system (45, 54). Notably, chemical sympathetic blockade markedly improved the survival rate, attenuated body weight loss, and reduced pulmonary cytokine expression in liraglutide-treated mice with bleomycin-induced lung injury. Our findings are also consistent with reports that the deleterious effects observed with exendin-4 on lung inflammation in mice with extensive thermal injury are attenuated by sympathetic nervous system blockade (55). Collectively, these results highlight emerging roles for the sympathetic nervous system in transducing deleterious actions of GLP-1R agonists in mice with experimental lung injury.

Our studies of mice with influenza virus infection were prompted in part by data highlighting the role of gut microbial signals in modulating the pulmonary immune

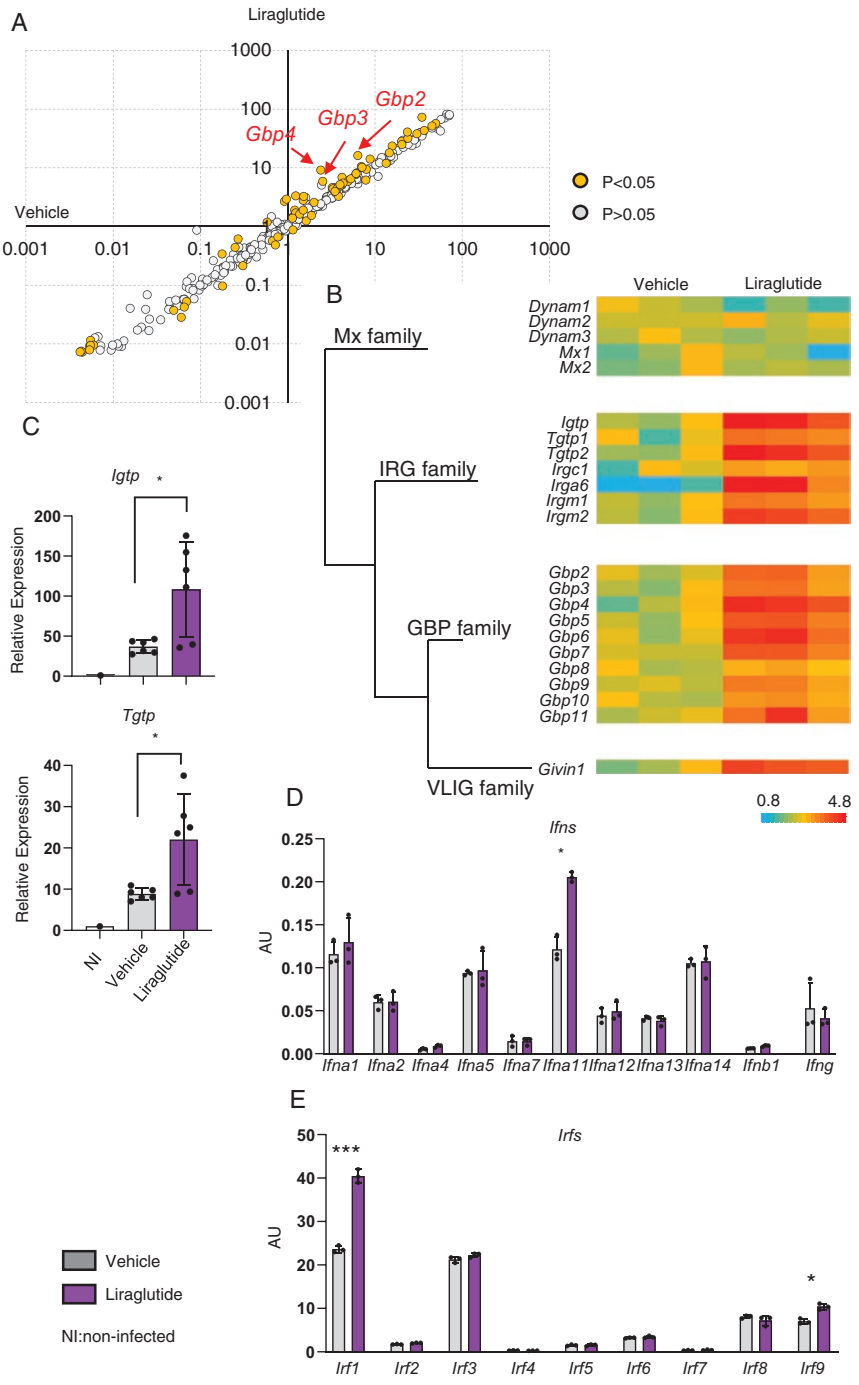

Figure 6. Liraglutide increases the expression of guanylate-binding proteins (GBPs). A, Logarithm of the expression level of interferon-stimulated genes (ISGs) in the lung 1 day after influenza virus infection in the liraglutide- and vehicle-administration group. B, Heat map showing GBP expression 1 day after influenza virus infection. C, *Igtp* and *Tgtp2* messenger RNA transcripts in the lung 1 day after influenza virus infection. D, Interferon gene expression 1 day after influenza virus infection (each n = 3). E, Interferon regulatory factor 1 (IRF) gene expression 1 day after influenza virus infection (each n = 3). All values represent mean ± SEM. A, C, D, and E, **P* less than .05. ***P* less than .01 by nonpaired *t* test. *Ifna*, interferon α; *Ifnb*, interferon β; *Ifng*, interferon γ; NI: noninfected.

response to influenza infection (56). Intriguingly, GLP-1R agonists have been reported to reduce influenza virus infection in a meta-analysis of observational clinical studies (57). In our mouse influenza experiments, liraglutide improved survival and suppressed inflammation, findings associated with a reduction in influenza virus load. Gene pathway analysis suggested that GLP-1R signaling activates interferon-related signals, consistent with extensive data implicating interferon-inducible GTPases as key components of the immune response to viruses and bacteria (4, 7, 58). Intriguingly, liraglutide upregulated expression of the GLP-1R in circulating white blood cells from

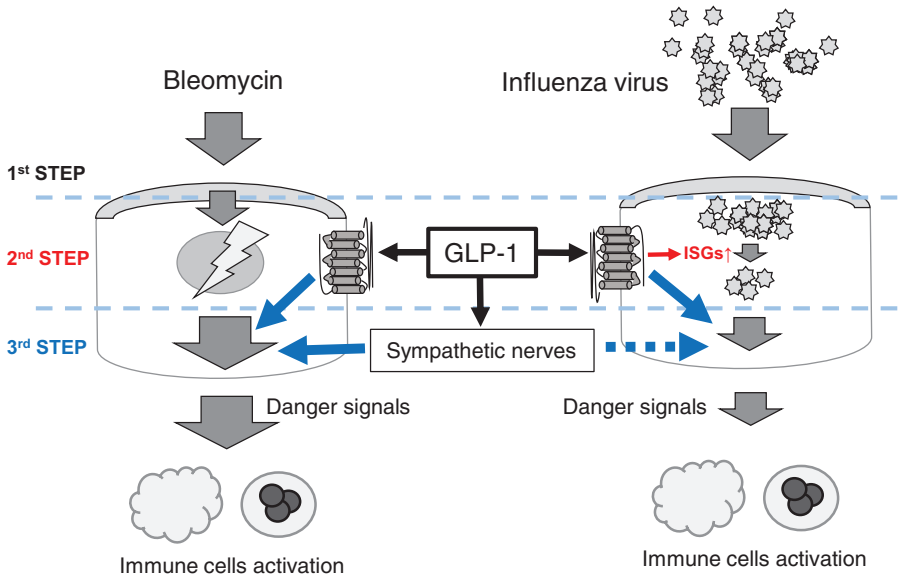

Figure 7. Conceptual models of glucagon-like peptide 1 (GLP-1) and defense against influenza virus infection. First step: Epithelial cells act as a physical barrier (whether GLP-1 is involved was not investigated in this study). Second step: GLP-1 reduces pathogens by expressing interferon-stimulated genes (ISGs) in the alveolar cells. Third step: GLP-1 activates immune cells and eliminates pathogens by enhancing danger signaling either directly to alveolar epithelial cells or via the sympathetic nervous system.

people with chronic obstructive pulmonary disease, and enhanced interferon-γ production from phytohemagglutinin-stimulated human mononuclear cells cultured ex vivo (59). Hence, our present findings support the concept of GLP-1R agonists modulating anti-inflammatory responses in experimental viral infection through augmentation of the endogenous interferon response.

The possibility that GLP-1 may alternatively enhance or suppress inflammation, depending on the model system, and the timing and duration of activated GLP-1 signaling, has been previously established. Indeed, we previously demonstrated that acute administration of exendin-4 to healthy mice rapidly and transiently upregulated the expression of multiple cytokine genes as well as genes encoding antimicrobial proteins in the jejunum (14). Exendin-4 also upregulated the expression of proinflammatory and antimicrobial genes in the distal gut of mice with dextran sulfate–induced colitis. In contrast, activation of GLP-1R signaling suppressed cytokine activation in intestinal epithelial lymphocytes (14), and extensive literature supports a sustained anti-inflammatory effect of GLP-1R agonists in multiple cell types and tissues (16, 20, 60). Collectively, these data support the concept that GLP-1 acutely augments the initial innate immune response to acute injury, while serving to suppress ongoing deleterious inflammatory responses in the setting of chronic inflammation.

The concept of a gut-lung axis has been proposed (10) linking the intestinal environment, gut inflammation, and the pathophysiology of lung disorders (61). Current dogma highlights the importance of gut microbiota and microbial metabolites such as short-chain fatty acids as key components of the gut-lung axis (10). As outlined earlier, L cells also serve as pathogen sensors, secreting GLP-1 in response to microbial-derived metabolites, LPS, or short-chain fatty acids (16, 62, 63). Taken together, our findings extend the importance of understanding the impact of GLP-1R signaling in the context of lung inflammation and suggest that gut-derived peptides such as GLP-1 may be additional components of the emerging gut-lung axis.

The present findings have several limitations. First, we were unable to identify the precise cell types expressing the GLP-1R within or external to the lung, essential for transducing key signals affecting the pathophysiology of lung injury after bleomycin or influenza virus infection. Although there is a clear difference in tissue inflammation and survival after treatment with liraglutide, we have examined changes only in gene expression for cytokines and other factors, and future studies would ideally analyze for protein levels of key mediators in similar experiments. Moreover, we used *Glp1r*$^{-/-}$ mice with germline loss of the GLP-1R, which may have evolved compensatory mechanisms throughout development that masked the potential biology arising from acute loss of GLP-1R signaling in adult mice. Furthermore, we did not use littermates in wild-type and GLP-1R KO mice in our experiments, but the use of littermates is ideal. We observed a greater extent of bleomycin-induced lung injury using 0.2 mg/kg of liraglutide, whereas previous studies have demonstrated reduced inflammation and decreased fibrosis in mice with bleomycin-induced pulmonary inflammation after treatment with a 10-fold higher dose of liraglutide (64). Hence, further studies will be required to understand the precise-dose response relations for the

negative vs beneficial effects of GLP-1R agonism in this model of sterile lung injury. Nevertheless, our studies demonstrating that activation of GLP-1R signaling attenuates virus-induced lung injury in preclinical studies may have translational relevance for ongoing studies examining interventions suitable for attenuating lung injury in the context of diabetes and infectious lung injury, as exemplified by SARS-CoV-2 infection (26).

Acknowledgments

We thank Susumu Seino for critical reading the manuscript and for helpful discussion; Kaoru Sakamoto, Kayoko Kagaya, Hiromi Fujishima, and Midori Matsuhashi for excellent technical support; Seiki Fujiwara for technical assistance with influenza virus experiments; and Masahide Takeda for the advice about the experiment of bleomycin-induced lung injury.

Financial Support: This work was supported in part by Grants-in-Aid for Scientific Research from the Japan Society for the Promotion of Science (Grant No. 18H03171), Japan Agency for Medical Research and Development (Grant No. JP18ek0210111), the scientific research grant from the Japan Association for Diabetes Education and Care, and Front Runner of Future Diabetes Research by the Japan Foundation for Applied Enzymology. D.J.D. is supported by the Canadian Institutes of Health Research (Grant No. 154321), a Banting and Best Diabetes Centre–Novo Nordisk Chair, and the Novo Nordisk Foundation–Mt. Sinai Hospital Fund in gut hormone biology.

Author Contributions: T.Sa. designed the study, performed the majority of the experiments, analyzed the data, and wrote the manuscript; T.Sh. performed the experiments; Y.I. provided expert advice about the influenza virus infection experiment and environment, performed the experiments about the influenza virus, and wrote the manuscript; H.F, D.J.D, and Y.S provided helpful suggestions on experimental design and provided critical reading of the manuscript; D.J.D wrote the manuscript and provided the *Glp1r*-deficient mice; Y.Y. designed the study, performed experiments, supervised the project, and co-wrote the manuscript.

Additional Information

Correspondence: Yuichiro Yamada, MD, PhD, Kansai Electric Power Medical Research Institute, Department of Endocrinology, Diabetes and Geriatric Medicine, Division of Diabetes, Clinical Nutrition, and Endocrinology, 2-1-7 Fukushima, Fukushima-ku, Osaka 553-0003, Japan. E-mail: yyamada-dm@umin.ac.jp.

Disclosure Summary: The authors have declared that no direct conflict of interest exists. D.J.D. is a speaker or consultant for Intarcia, Kallyope, Merck, Novo Nordisk, and receives investigator-initiated support via Mt. Sinai Hospital from Takeda and Novo Nordisk for preclinical studies of glucagon-like peptides.

Data Availability: All data generated or analyzed during this study are included in this published article or in the data repositories listed in "References."

References

1. Blake KJ, Jiang XR, Chiu IM. Neuronal regulation of immunity in the skin and lungs. *Trends Neurosci.* 2019;**42**(8):537-551.
2. Leiva-Juárez MM, Kolls JK, Evans SE. Lung epithelial cells: therapeutically inducible effectors of antimicrobial defense. *Mucosal Immunol.* 2018;**11**(1):21-34.
3. Ganesan S, Comstock AT, Sajjan US. Barrier function of airway tract epithelium. *Tissue Barriers.* 2013;**1**(4):e24997.
4. Tretina K, Park ES, Maminska A, MacMicking JD. Interferon-induced guanylate-binding proteins: guardians of host defense in health and disease. *J Exp Med.* 2019;**216**(3):482-500.
5. Wallace WA, Fitch PM, Simpson AJ, Howie SE. Inflammation-associated remodelling and fibrosis in the lung—a process and an end point. *Int J Exp Pathol.* 2007;**88**(2):103-110.
6. Michalska A, Blaszczyk K, Wesoly J, Bluyssen HAR. A positive feedback amplifier circuit that regulates interferon (IFN)-stimulated gene expression and controls type I and type II IFN responses. *Front Immunol.* 2018;**9**:1135.
7. Pilla-Moffett D, Barber MF, Taylor GA, Coers J. Interferon-inducible GTPases in host resistance, inflammation and disease. *J Mol Biol.* 2016;**428**(17):3495-3513.
8. Mindt BC, Fritz JH, Duerr CU. Group 2 innate lymphoid cells in pulmonary immunity and tissue homeostasis. *Front Immunol.* 2018;**9**:840.
9. Jänig W. Sympathetic nervous system and inflammation: a conceptual view. *Auton Neurosci.* 2014;**182**:4-14.
10. Dang AT, Marsland BJ. Microbes, metabolites, and the gut-lung axis. *Mucosal Immunol.* 2019;**12**(4):843-850.
11. Anand S, Mande SS. Diet, microbiota and gut-lung connection. *Front Microbiol.* 2018;**9**:2147.
12. Tolhurst G, Heffron H, Lam YS, et al. Short-chain fatty acids stimulate glucagon-like peptide-1 secretion via the G-protein-coupled receptor FFAR2. *Diabetes.* 2012;**61**(2):364-371.
13. Greiner TU, Bäckhed F. Microbial regulation of GLP-1 and L-cell biology. *Mol Metab.* 2016;**5**(9):753-758.
14. Yusta B, Baggio LL, Koehler J, et al. GLP-1R agonists modulate enteric immune responses through the intestinal intraepithelial lymphocyte GLP-1R. *Diabetes.* 2015;**64**(7):2537-2549.
15. He S, Kahles F, Rattik S, et al. Gut intraepithelial T cells calibrate metabolism and accelerate cardiovascular disease. *Nature.* 2019;**566**(7742):115-119.
16. Drucker DJ. The cardiovascular biology of glucagon-like peptide-1. *Cell Metab.* 2016;**24**(1):15-30.
17. Lebrun LJ, Lenaerts K, Kiers D, et al. Enteroendocrine L cells sense LPS after gut barrier injury to enhance GLP-1 secretion. *Cell Rep.* 2017;**21**(5):1160-1168.
18. Fujita H, Morii T, Fujishima H, et al. The protective roles of GLP-1R signaling in diabetic nephropathy: possible mechanism and therapeutic potential. *Kidney Int.* 2014;**85**(3):579-589.
19. Helmstädter J, Frenis K, Filippou K, et al. Endothelial GLP-1 (glucagon-like peptide-1) receptor mediates cardiovascular protection by liraglutide in mice with experimental arterial hypertension. *Arterioscler Thromb Vasc Biol.* 2020;**40**(1):145-158.
20. Lee YS, Jun HS. Anti-inflammatory effects of GLP-1-based therapies beyond glucose control. *Mediators Inflamm.* 2016;**2016**:3094642.
21. Lankat-Buttgereit B, Göke R, Fehmann HC, Richter G, Göke B. Molecular cloning of a cDNA encoding for the GLP-1 receptor expressed in rat lung. *Exp Clin Endocrinol.* 1994;**102**(4):341-347.

22. Wei Y, Mojsov S. Distribution of GLP-1 and PACAP receptors in human tissues. *Acta Physiol Scand*. 1996;**157**(3):355-357.
23. Yamada Y, Tsukiyama K, Sato T, Shimizu T, Fujita H, Narita T. Novel extrapancreatic effects of incretin. *J Diabetes Investig*. 2016;**7**(Suppl 1):76-79.
24. Vara E, Arias-Díaz J, Garcia C, Balibrea JL, Blázquez E. Glucagon-like peptide-1(7-36) amide stimulates surfactant secretion in human type II pneumocytes. *Am J Respir Crit Care Med*. 2001;**163**(4):840-846.
25. Benito E, Blazquez E, Bosch MA. Glucagon-like peptide-1-(7-36) amide increases pulmonary surfactant secretion through a cyclic adenosine 3′,5′-monophosphate-dependent protein kinase mechanism in rat type II pneumocytes. *Endocrinology*. 1998;**139**(5):2363-2368.
26. Drucker DJ. Coronavirus infections and type 2 diabetes–shared pathways with therapeutic implications. *Endocr Rev*. 2020;**41**(3):457-470.
27. Scrocchi LA, Brown TJ, MaClusky N, et al. Glucose intolerance but normal satiety in mice with a null mutation in the glucagon-like peptide 1 receptor gene. *Nat Med*. 1996;**2**(11):1254-1258.
28. Ji WJ, Ma YQ, Zhou X, et al. Temporal and spatial characterization of mononuclear phagocytes in circulating, lung alveolar and interstitial compartments in a mouse model of bleomycin-induced pulmonary injury. *J Immunol Methods*. 2014;**403**(1-2):7-16.
29. Cheng T, Liu Q, Zhang R, et al. Lysyl oxidase promotes bleomycin-induced lung fibrosis through modulating inflammation. *J Mol Cell Biol*. 2014;**6**(6):506-515.
30. Kikuchi N, Ishii Y, Morishima Y, et al. Aggravation of bleomycin-induced pulmonary inflammation and fibrosis in mice lacking peroxiredoxin I. *Am J Respir Cell Mol Biol*. 2011;**45**(3):600-609.
31. Okazaki M, Yamada Y, Nishimoto N, Yoshizaki K, Mihara M. Characterization of anti-mouse interleukin-6 receptor antibody. *Immunol Lett*. 2002;**84**(3):231-240.
32. Hartman MH, Vreeswijk-Baudoin I, Groot HE, et al. Inhibition of interleukin-6 receptor in a murine model of myocardial ischemia-reperfusion. *PLoS One*. 2016;**11**(12):e0167195.
33. Akita K, Isoda K, Sato-Okabayashi Y, et al. An interleukin-6 receptor antibody suppresses atherosclerosis in atherogenic mice. *Front Cardiovasc Med*. 2017;**4**:84.
34. Yaoita T, Sasaki Y, Yokozawa J, et al. Treatment with anti-interleukin-6 receptor antibody ameliorates intestinal polyposis in *ApcMin*/+ mice under high-fat diet conditions. *Tohoku J Exp Med*. 2015;**235**(2):127-134.
35. Morita M, Kuba K, Ichikawa A, et al. The lipid mediator protectin D1 inhibits influenza virus replication and improves severe influenza. *Cell*. 2013;**153**(1):112-125.
36. *RRID; AB_2877061*.
37. *RRID; CVCL_3751*.
38. *Akita University institutional repository system*. Deposited November 9, 2020. http://hdl.handle.net/10295/00005149
39. Shimizu T, Sato T, Tsukiyama K, et al. Food intake affects sperm-egg fusion through the GIP/PSG17 axis in mice. *Endocrinology*. 2017;**158**(7):2134-2144.
40. Li L, Yu Q, Hu JM. Expression of epidermal growth factor receptor and the oncogene c-erbB2 on pulmonary fibrosis induced by bleomycin in rats [article in Chinese]. *Zhonghua Lao Dong Wei Sheng Zhi Ye Bing Za Zhi*. 2011;**29**(7):537-540.
41. Ishii Y, Fujimoto S, Fukuda T. Gefitinib prevents bleomycin-induced lung fibrosis in mice. *Am J Respir Crit Care Med*. 2006;**174**(5):550-556.
42. Gurujeyalakshmi G, Wang Y, Giri SN. Taurine and niacin block lung injury and fibrosis by down-regulating bleomycin-induced activation of transcription nuclear factor-kappaB in mice. *J Pharmacol Exp Ther*. 2000;**293**(1):82-90.
43. Wikenheiser KA, Vorbroker DK, Rice WR, et al. Production of immortalized distal respiratory epithelial cell lines from surfactant protein C/simian virus 40 large tumor antigen transgenic mice. *Proc Natl Acad Sci U S A*. 1993;**90**(23):11029-11033.
44. Saito F, Tasaka S, Inoue K, et al. Role of interleukin-6 in bleomycin-induced lung inflammatory changes in mice. *Am J Respir Cell Mol Biol*. 2008;**38**(5):566-571.
45. Lorenz M, Lawson F, Owens D, et al. Differential effects of glucagon-like peptide-1 receptor agonists on heart rate. *Cardiovasc Diabetol*. 2017;**16**(1):6.
46. Pérez-Tilve D, González-Matías L, Aulinger BA, et al. Exendin-4 increases blood glucose levels acutely in rats by activation of the sympathetic nervous system. *Am J Physiol Endocrinol Metab*. 2010;**298**(5):E1088-E1096.
47. Yamamoto H, Lee CE, Marcus JN, et al. Glucagon-like peptide-1 receptor stimulation increases blood pressure and heart rate and activates autonomic regulatory neurons. *J Clin Invest*. 2002;**110**(1):43-52.
48. Varin EM, Mulvihill EE, Baggio LL, et al. Distinct neural sites of GLP-1R expression mediate physiological versus pharmacological control of incretin action. *Cell Rep*. 2019;**27**(11):3371-3384.e3.
49. Schoggins JW, Wilson SJ, Panis M, et al. A diverse range of gene products are effectors of the type I interferon antiviral response. *Nature*. 2011;**472**(7344):481-485.
50. Chimerel C, Emery E, Summers DK, Keyser U, Gribble FM, Reimann F. Bacterial metabolite indole modulates incretin secretion from intestinal enteroendocrine L cells. *Cell Rep*. 2014;**9**(4):1202-1208.
51. Nguyen AT, Mandard S, Dray C, et al. Lipopolysaccharides-mediated increase in glucose-stimulated insulin secretion: involvement of the GLP-1 pathway. *Diabetes*. 2014;**63**(2):471-482.
52. Lebherz C, Schlieper G, Möllmann J, et al. GLP-1 levels predict mortality in patients with critical illness as well as end-stage renal disease. *Am J Med*. 2017;**130**(7):833-841.e3.
53. Zhu T, Li C, Zhang X, et al. GLP-1 analogue liraglutide enhances SP-A expression in LPS-induced acute lung injury through the TTF-1 signaling pathway. *Mediators Inflamm*. 2018;**2018**:3601454.
54. Padro CJ, Sanders VM. Neuroendocrine regulation of inflammation. *Semin Immunol*. 2014;**26**(5):357-368.
55. Ji XJ, Hao JW, Li GL, et al. Exendin-4 exacerbates burn-induced morbidity in mice by activation of the sympathetic nervous system. *Mediators Inflamm*. 2019;**2019**:2750528.
56. Ichinohe T, Pang IK, Kumamoto Y, et al. Microbiota regulates immune defense against respiratory tract influenza A virus infection. *Proc Natl Acad Sci U S A*. 2011;**108**(13):5354-5359.
57. Li WX, Gou JF, Tian JH, Yan X, Yang L. Glucagon-like peptide-1 receptor agonists versus insulin glargine for type 2 diabetes mellitus: a systematic review and meta-analysis of randomized controlled trials. *Curr Ther Res Clin Exp*. 2010;**71**(4):211-238.

58. Kim BH, Shenoy AR, Kumar P, Bradfield CJ, MacMicking JD. IFN-inducible GTPases in host cell defense. *Cell Host Microbe*. 2012;**12**(4):432-444.
59. Huang J, Yi H, Zhao C, et al. Glucagon-like peptide-1 receptor (GLP-1R) signaling ameliorates dysfunctional immunity in COPD patients. *Int J Chron Obstruct Pulmon Dis*. 2018;**13**:3191-3202.
60. Müller TD, Finan B, Bloom SR, et al. Glucagon-like peptide 1 (GLP-1). *Mol Metab*. 2019;**30**:72-130.
61. Dumas A, Bernard L, Poquet Y, Lugo-Villarino G, Neyrolles O. The role of the lung microbiota and the gut-lung axis in respiratory infectious diseases. *Cell Microbiol*. 2018;**20**(12):e12966.
62. Kaji I, Karaki S, Kuwahara A. Short-chain fatty acid receptor and its contribution to glucagon-like peptide-1 release. *Digestion*. 2014;**89**(1):31-36.
63. Christiansen CB, Gabe MBN, Svendsen B, Dragsted LO, Rosenkilde MM, Holst JJ. The impact of short-chain fatty acids on GLP-1 and PYY secretion from the isolated perfused rat colon. *Am J Physiol Gastrointest Liver Physiol*. 2018;**315**(1):G53-G65.
64. Gou S, Zhu T, Wang W, Xiao M, Wang XC, Chen ZH. Glucagon like peptide-1 attenuates bleomycin-induced pulmonary fibrosis, involving the inactivation of NF-κB in mice. *Int Immunopharmacol*. 2014;**22**(2):498-504.

Supplemental Figure 1

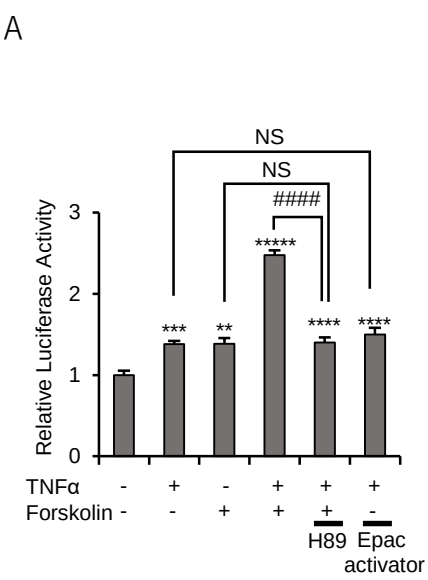

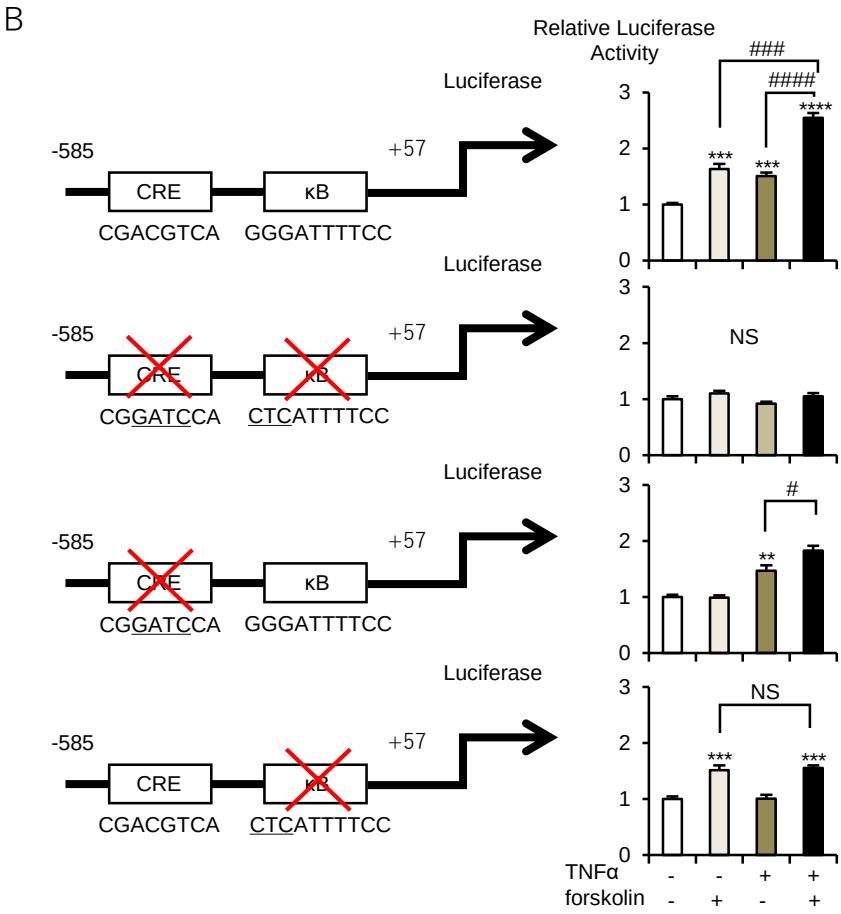

Supplemental Figure 2

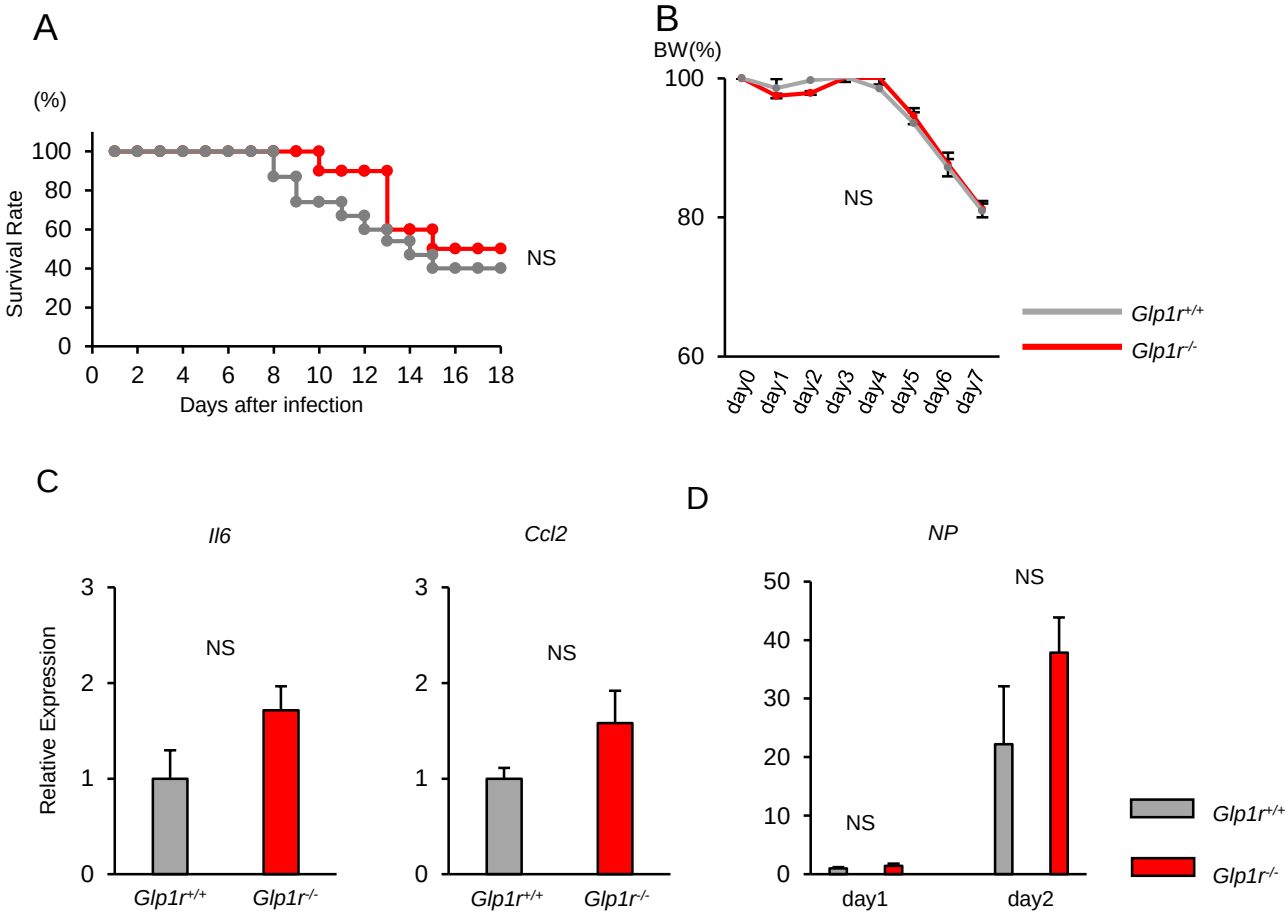

Supplemental Figure 3

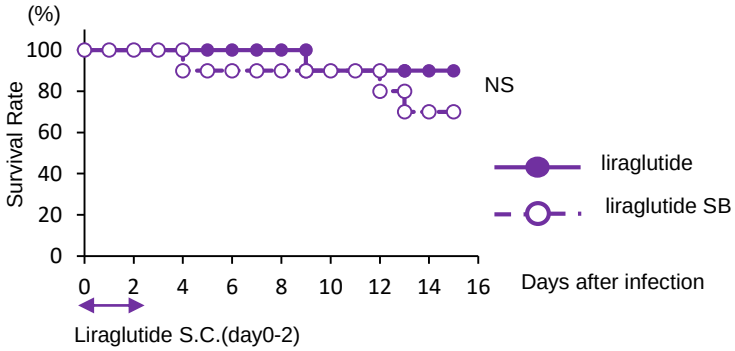

Supplemental Figure 4

A

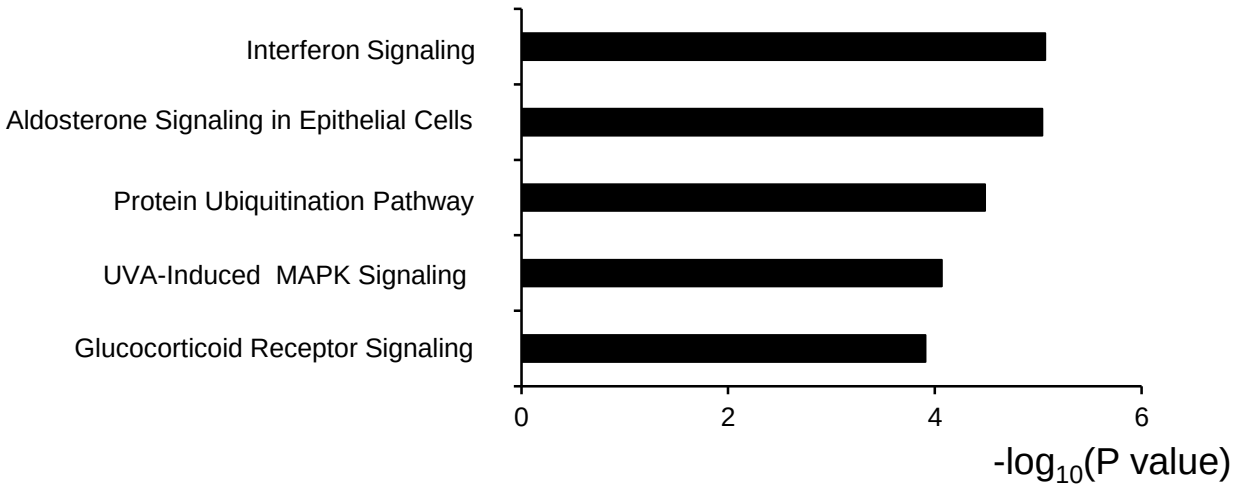

B

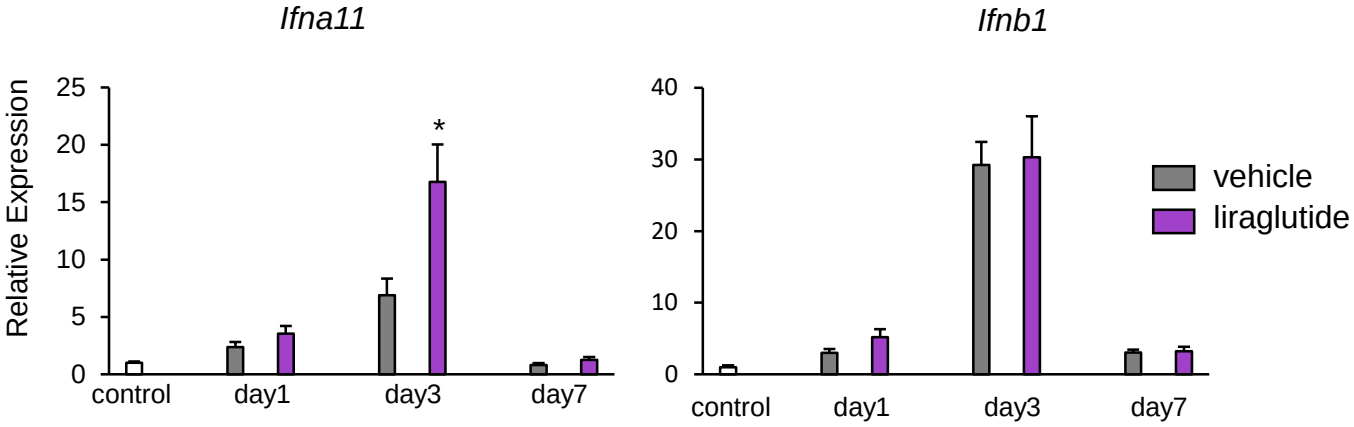

Supplemental Figure 5

A

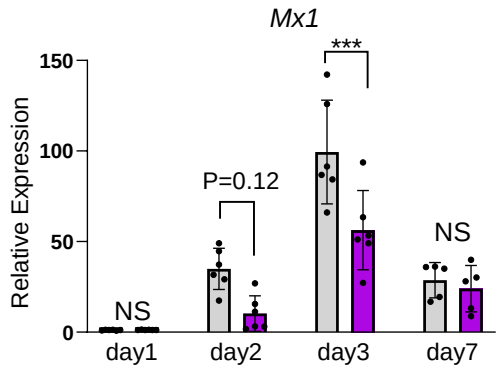

B

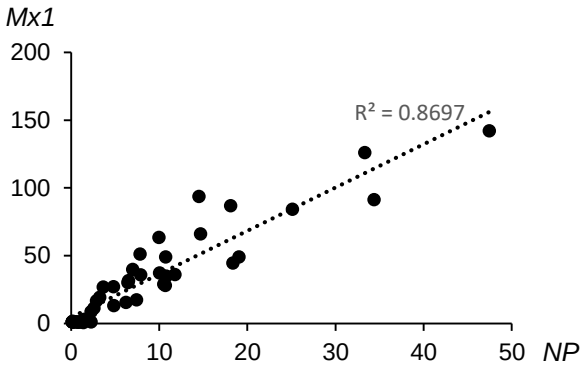

C

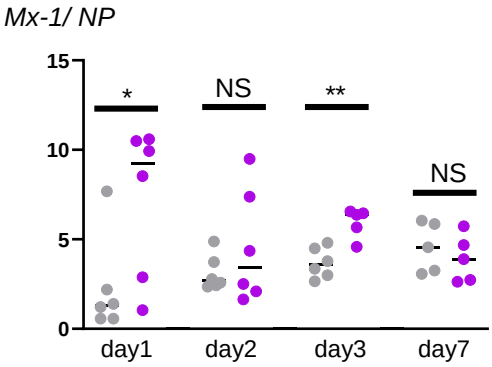

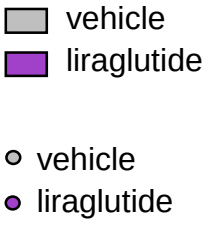

Supplemental Table

Gene	Forward	Reverse
Glp-1r	ctgcccagcaacaccagt	cagtcggcagcctagagagt
full length *Glp-1r*	gtaccacggtgtccctctca	cctgtgtccttcaccttcccta
Cd11c	atggagcctcaagacaggac	ggatctgggatgctgaaatc
Cd206	ccacagcattgaggagtttg	acagctcatcatttggctca
Sftpc	ggtcctgatggagagtccac	gatgagaaggcgtttgaggt
Il-6	tgatggatgctaccaaactgg	ttcatgtactccaggtagctatgg
Ccl-2	catccacgtgttggctca	gatcatcttgctggtgaatgagt
Il-1beta	agttgacggaccccaaaag	agctggatgctctcatcagg
Cxcl-2	aaaatcatccaaaagatactgaacaa	ctttggttcttccgttgagg
Tgfbeta	tggagcaacatgtggaactc	cagcagccggttaccaag
Egfr	ttggaatcaattttacaccgaat	gttcccacacagtgacacca
Np	gattggtggaattggacgat	agagcaccattctctctatt
Igtp	cggagagctgtggagagaga	gccatgtttatgaaaagtgtaaaagtc
Tgtp	ccagatcaaggtcaccactg	gagatgattttgctttccctttt
Ifnb	ctcactttgcccttagtcaatatg	tcaaaggctgcagtgagaatg
Ifna11	aggactttggattccccttg	agggatggattgagccttct
18s	ctcaacacgggaaacctcac	cgctccaccaactaagaacg

Supplementary Figure 1

(A) Promoter activity of IL-6 under various conditions in MLE12. Each drug was used as described in MATERIALS AND METHODS.(B)IL-6 promoter activity after disruption of CREB and NFkB binding lesion in MLE12. All values represent mean ± SEM. **P<0.01, ***P<0.001, ****P<0.0001 versus absence of TNFα and forskolin. # P<0.05, ###P<0.001, ####P<0.0001. (each n=6) by one-way ANOVA with multiple comparison test.

Supplementary Figure 2

(A)Survival rates and (B)body weight change of the *Glp1r*$^{+/+}$ mice and *Glp1r*$^{-/-}$ mice after influenza virus infection (*Glp1r*$^{+/+}$ n=15, *Glp1r*$^{-/-}$ n=10). (C)Cytokines and chemokines gene expression in the lung of *Glp1r*$^{+/+}$ mice and *Glp1r*$^{-/-}$ mice 2days after influenza virus infection. (each n=5) (D)NP protein gene expression in the lung of *Glp1r*$^{+/+}$ mice and *Glp1r*$^{-/-}$ mice after influenza virus infection. (each n=5) All values represent mean ± SEM. *P<0.05, **P<0.01, NS: not statistically significant by non-paired t-test (B, C, D) and Log-Lank test (A).

Supplementary Figure 3

The effect of sympathetic block on the survival of the influenza infected mice with liraglutide. NS: not statistically significant by Log-Lank test .

Supplementary Figure 4

(A) Pathway analysis based on the gene expression in the lung 1 day after influenza

administration. (B) Interferons gene expression after influenza virus infection. All values represent mean ± SEM.(NI: n=3 the other: n=5～6) *P<0.05 by non-paired t-test (B).

Supplementary Figure 5

(A)*Mx1* mRNA transcripts in the lung after influenza infection with or without iraglutide (from the left n=6: 6: 6: 6: 6: 6: 5: 5). (B) Correlation between *NP* and *Mx1* gene expression after influenza virus infection (day1,2,3,7). *Mx1/NP* gene expression ratio after influenza virus infection (from the left n=6: 6: 6: 6: 6: 5: 5: 5). *P<0.05, **P<0.01, ***P<0.001 by one-way ANOVA with multiple comparison test (A) and Mann Whitney test (C).